Statistica Sinica Preprint No: SS-2018-0214	
Title	Testing First-Order Spherical Symmetry of Spatial Point Processes
Manuscript ID	SS-2018-0214
URL	http://www.stat.sinica.edu.tw/statistica/
DOI	10.5705/ss.202018.0214
Complete List of Authors	Tonglin Zhang and Jorge Mateu
Corresponding Author	Tonglin Zhang
E-mail	tlzhang@purdue.edu

Statistica Sinica: Preprint
doi:10.5705/ss.202018.0214

Testing First-Order Spherical Symmetry of Spatial Point Processes

Tonglin Zhang and Jorge Mateu

Purdue University and Universitat Jaume I

Abstract: This study proposes a Kolmogorov–Smirnov–type test to assess the spherical symmetry of the first-order intensity function of a spatial point process (SPP). Spherical symmetry, which is an important assumption in the well known epidemic-type aftershock sequence (ETAS) model, means that the intensity function of an SPP is invariant under a spherical transformation in a Euclidean space. An important property of first-order spherical symmetry is that the expected number of points within a sector region is proportional to the angle measure of the region. This provides a way to construct our test statistic. The asymptotic distribution of the test statistic is obtained under the framework of increasing domain asymptotics, with weak dependence. We show that the resulting test statistic converges weakly to the absolute maximum of a zero mean Gaussian process under the null hypothesis, and that it is also consistent under the alternative hypothesis. A simulation study shows that the type-I error probability of the test is close to the significance level, and the power increases to one as the magnitude of nonspherical symmetry increases. An application of the ETAS model to earthquakes in Japan shows that the first-order spherical symmetry

Statistica Sinica: Preprint
doi:10.5705/ss.202018.0214

assumption can be approximately accepted.

Key words and phrases: Gaussian processes; Intensity functions; Kolmogorov–Smirnov test; Polar transformation; Spatial point processes (SPPs); Spherical symmetry.

1. Introduction

Spatial point processes (SPPs) are widely applied in a variety of scientific disciplines, including forestry (Stoyan, 1994), epidemiology (Diggle, 2006), wildfires (Peng, Schoenberg, and Woods, 2005), and earthquakes (Ogata, 1988). In the literature, an SPP is treated as a pattern of points for locations of random events developed in a complete separable metric space or a bounded subset of the space. Point distributions and dependence structures are modeled by intensity functions (Diggle, 2003). The simplifying assumptions of stationarity and isotropy have been developed to make the analysis of SPPs convenient. Various well known tools have been proposed, including the K-function (Ripley, 1976), L-function (Besag, 1977), and pair correlation function (Stoyan and Stoyan, 1996). Because of its importance, several methods have been proposed to assess stationarity (Guan, 2008; Zhang and Zhou, 2014). However, a recent interest is to model SPPs under nonstationarity (Møller and Waagepetersen, 2007). An important concept called second-order intensity-reweighted stationarity (SOIRS) has been

Statistica Sinica: Preprint
doi:10.5705/ss.202018.0214

proposed (Baddeley, Møller, and Waagepetersen, 2000). The concept is powerful in the joint analysis of the first-order and second-order intensity functions under nonstationarity. With the aid of SOIRS, a number of methods for nonstationary SPPs have been proposed (Guan and Shen, 2010; Henrys and Brown, 2009; Waagepetersen, 2007).

SOIRS provides the relationship between the first-order and the second-order intensity functions, but does not specify any assumptions for the first-order intensity function; therefore, such assumptions can be proposed independently. This allows us to develop models for the first-order intensity function only, while simultaneously addressing the second-order properties. Here, relevant methods include parametric and nonparametric estimation (Diggle, 1985), Bayesian estimation (Myllymäki and Penttinen, 2009), proportionality (Zhang and Zhuang, 2017), and separability (Zhang, 2014, 2017). Although first-order intensity functions are useful in practice, an important question about whether they have a spherically symmetric structure remains unanswered. The purpose of this study is to develop a formal statistical test to address this problem.

Spherical symmetry is an important assumption of the well known epidemic-type aftershock sequence (ETAS) model, one of the earliest point process models created for clustered events. The ETAS is a parametric model defined by a conditional intensity function for mainshock and aftershock earthquakes. It

Statistica Sinica: Preprint
doi:10.5705/ss.202018.0214

was originally developed for earthquakes (Zhuang, Ogata, and Vere-Jones, 2002), and later extended to infectious diseases (Meyer and Held, 2014) and invasive species (Balderama, et. al, 2012). In the ETAS model, events in each aftershock cluster are independently produced by their corresponding mainshock earthquakes (ancestors). The size of the aftershock cluster depends on the magnitude of its ancestor. If there is only one extremely large ancestor, then within a certain period, the entire earthquake pattern is dominated by the ancestor and its aftershocks. Therefore, our approach can be used to justify the assumptions of the ETAS model, although our interest lies beyond this topic.

Our approach is motivated by the classical tests for spherical symmetry of multivariate distributions. Spherically symmetric distributions are natural extensions of the multivariate standard normal distribution. The spherically symmetric multivariate distribution, which can be traced back to Hall, Watson, and Cabrera (1987), is well known in the literature. The focus is either estimation (Brandwein and Strawderman, 1991) or hypothesis testing (Henze, Hlávka, and Meintanis, 2014), based on an identically and independently distributed (i.i.d.) sample. Because of the existence of dependence, these approaches cannot be used to assess the spherical symmetry of SPPs. Therefore, new approaches are needed.

We propose a Kolmogorov–Smirnov–type statistic to assess spherical symmetry. The dependence structure is described by a scale parameter in the test

Statistica Sinica: Preprint
doi:10.5705/ss.202018.0214

statistic. The p-value is calculated using its asymptotic null distribution. We evaluate the properties of our test by means of simulations and applications. In the simulations, we study type-I error probabilities and power. We conclude that the type-I error probabilities are always close to the significance level, and that the power function always increases to one as the magnitude of the nonspherical symmetry increases. For illustration, we apply our test to an earthquake data set. We conclude that the spherical symmetry assumption is correct at the beginning of the occurrence of a great earthquake, in general, indicating that the ETAS model can capture major characteristics of earthquake aftershock patterns.

To the best of our knowledge, our approach is the first formal test for the spherical symmetry of SPPs. Because the test statistic is purely nonparametric, our approach can be easily implemented to study the properties of the spherical symmetry of an SPP, without needing to specify a model for the intensity function. Furthermore, because the computation of the test statistic does not involve estimates of the intensity function, our approach avoids the complicated nonparametric estimation problem.

The article is organized as follows. In Section 2, we propose our test statistic and derive its asymptotic null distribution and power functions. In Section 3, we evaluate the performance of our test statistic using Monte Carlo simulations. We apply our approach to Japan earthquake data in Section 4. Section 5 concludes

Statistica Sinica: Preprint
doi:10.5705/ss.202018.0214

the paper.

2. Methodology

We define SPPs in Section 2.1, discuss the concept of spherical symmetry in Section 2.2, propose our test for first-order spherical symmetry in Section 2.3, and derive its asymptotic null distribution in Section 2.4.

2.1 Spatial Point Processes

An SPP $\mathcal{N}(W)$ in $W \in \mathscr{B}(\mathbb{R}^d)$ is composed of random points in W. It can be treated as the restriction of $\mathcal{N}$, the SPP on the entire $\mathbb{R}^d$, with points only observed in W, implying that points of $\mathcal{N}$ outside of W are unobserved. Let $\mathscr{B}$ and $\mathscr{B}(A)$ be collections of Borel sets of $\mathbb{R}^d$ and of a measurable $A \subseteq \mathbb{R}^d$, respectively. Then, $N(A)$, the number of points in A, is finite if A is bounded. The SPP $\mathcal{N}$ can be defined theoretically using the Janossy measure approach (Janossy, 1950) or the counting measure approach (Daley and Vere-Jones, 2003). The former is based on distribution functions. The latter is based on intensity functions. The two approaches have been shown to be theoretically equivalent in the literature (Moyal, 1962), and the latter is more popular than the former. Therefore, we only review the second approach.

The counting measure approach defines the kth-order intensity function

Statistica Sinica: Preprint
doi:10.5705/ss.202018.0214

of $\mathcal{N}$ as $\lambda_k(\mathbf{s}_1,\ldots,\mathbf{s}_k) = \lim_{\rho(U_{\mathbf{s}_i})\to 0, i=1,\ldots,k} \mathrm{E}\{\prod_{i=1}^k N(U_{\mathbf{s}_i})\}/\prod_{i=1}^k |U_{\mathbf{s}_i}|$, where $\mathbf{s}_1,\ldots,\mathbf{s}_k \in \mathbb{R}^d$ are distinct, $U_{\mathbf{s}}$ is a neighbor of $\mathbf{s}$, $|U_{\mathbf{s}}|$ is its Lebesgue measure, and $\rho(U_{\mathbf{s}})$ is the diameter of $U_{\mathbf{s}}$. The SPP $\mathcal{N}$ is said to be kth-order stationary if $\lambda_l(\mathbf{s}_1+\mathbf{h},\cdots,\mathbf{s}_l+\mathbf{h})$ does not depend on $\mathbf{h}$ for any positive $l \le k$ with distinct $\mathbf{s}_1,\cdots,\mathbf{s}_l \in \mathbb{R}^d$. In addition, the SPP is strong stationary if $\mathcal{N}$ is kth-order stationary for any positive integer k.

The mean structure of $\mathcal{N}$ is

$$\mu(A) = \mathrm{E}\{\mathcal{N}(A)\} = \int_A \lambda(\mathbf{s})d\mathbf{s}, \tag{1}$$

where $\lambda(\mathbf{s}) = \lambda_1(\mathbf{s})$ is the first-order intensity function. If $\mathcal{N}$ is first-order stationary, then $\lambda(\mathbf{s}) = c$ and $\mu(A) = c|A|$, where c is a positive constant. The covariance structure of $\mathcal{N}$ is $\mathrm{cov}\{\mathcal{N}(A_1),\mathcal{N}(A_2)\} = \int_{A_1}\int_{A_2}\{g(\mathbf{s}_1,\mathbf{s_2})-1\}\lambda(\mathbf{s}_1)\lambda(\mathbf{s}_2)d\mathbf{s_2}d\mathbf{s_1} + \mu(A_1\cap A_2)$, where $g(\mathbf{s}_1,\mathbf{s}_2) = \lambda_2(\mathbf{s}_1,\mathbf{s}_2)/\{\lambda(\mathbf{s}_1)\lambda(\mathbf{s}_2)\}$ is the pair correlation function. The variance structure of $\mathcal{N}$ is

$$\mathrm{V}\{\mathcal{N}(A)\} = \int_A \left\{\int_A [g(\mathbf{s}_1,\mathbf{s}_2)-1]\lambda(\mathbf{s}_2)d\mathbf{s}_2 + 1\right\}\lambda(\mathbf{s}_1)d\mathbf{s}_1. \tag{2}$$

If $g(\mathbf{s}_1,\mathbf{s}_2)$ depends only on $\mathbf{s}_1-\mathbf{s}_2$ or $\|\mathbf{s}_1-\mathbf{s}_2\|$, such that it can be expressed as $g(\mathbf{s}_1-\mathbf{s}_2)$ or $g(\|\mathbf{s}_1-\mathbf{s}_2\|)$, then $\mathcal{N}$ is called a second-order intensity-reweighted stationary SPP or a second-order intensity-reweighted isotropic SPP. This is an important concept for nonstationary SPPs (Baddeley, Møller, and Waagepetersen, 2000).

Statistica Sinica: Preprint
doi:10.5705/ss.202018.0214

2.2 Spherical Symmetry

We provide the concept of spherical symmetry for $\mathcal{N}$ on the entire $\mathbb{R}^d$, with $d \geq 2$, based on the counting measure approach. The concept means that intensity functions of $\mathcal{N}$ are invariant under a spherical transformation about a certain point in $\mathbb{R}^d$. It can be extended to a bounded region $W \subseteq \mathbb{R}^d$ if we treat $\mathcal{N}(W)$ as the set of observations.

Assume that $\lambda_k(\mathbf{s}_1, \cdots, \mathbf{s}_k)$ is well defined for any $k \leq n$. We say $\mathcal{N}$ is nth-order *spherically symmetric* if there exists an $\mathbf{s}_0 \in \mathbb{R}^d$, such that

$$\lambda_k(\mathbf{s}_1, \cdots, \mathbf{s}_k) = \lambda_k(\mathbf{s}_0 + \mathbf{U}(\mathbf{s}_1 - \mathbf{s}_0), \cdots, \mathbf{s}_0 + \mathbf{U}(\mathbf{s}_k - \mathbf{s}_0)), \tag{3}$$

for any $k \leq n$ and any orthogonal matrix $\mathbf{U}$ on $\mathbb{R}^d$. We say that $\mathcal{N}$ is *strongly spherically symmetric* if there exists an $\mathbf{s}_0 \in \mathbb{R}^d$, such that (3) holds for any $n \in \mathbb{N}$. An SPP $\mathcal{N}(W)$ is nth-order spherically symmetric or strongly spherically symmetric in a measurable $W \subseteq \mathbb{R}^d$ if it can be restricted by an nth-order spherically symmetric or strongly spherically symmetric $\mathcal{N}$ in $\mathbb{R}^d$.

Example 1. *Poisson SPPs. The kth-order intensity function of a Poisson SPP* $\mathcal{N}$ *is* $\lambda_k(\mathbf{s}_1, \cdots, \mathbf{s}_k) = \prod_{i=1}^{k} \lambda(\mathbf{s}_i)$. *If* N *follows a Poisson distribution with mean* κ, *then* $\lambda(\mathbf{s}) = \kappa f(\mathbf{s})$, *implying that* $\mathcal{N}$ *is strongly spherically symmetric if* $f(\mathbf{s})$ *is spherically symmetric about some* $\mathbf{s}_0$.

Example 2. *Poisson cluster SPPs. A Poisson cluster SPP* $\mathcal{N}$ *is derived by first*

Statistica Sinica: Preprint
doi:10.5705/ss.202018.0214

generating parent points from a Poisson SPP with intensity $\varphi(\mathbf{c})$*. Then, from each parent point, we generate* $Poisson(\eta)$ *number of offspring points, identically and independently, with density* $\psi(\mathbf{s}-\mathbf{c})$*, where* $\mathbf{c}$ *and* $\mathbf{s}$ *represent parent and offspring points, respectively. By Campbell's theorem, we have* $\lambda(\mathbf{s}) = \int_{\mathbb{R}^d} \eta\psi(\mathbf{s}-\mathbf{c})\varphi(\mathbf{c})d\mathbf{c}$ *and* $\lambda_2(\mathbf{s}_1,\mathbf{s}_2) = \int_{\mathbb{R}^d} \eta^2\psi(\mathbf{s}_1-\mathbf{c})\psi(\mathbf{s}_2-\mathbf{c})\varphi(\mathbf{c})d\mathbf{c}+\lambda(\mathbf{s}_1)\lambda(\mathbf{s}_2)$*. Thus,* $\mathcal{N}$ *is strongly spherically symmetric about* $\mathbf{s}_0$ *if* ψ *is spherically symmetric about* $\mathbf{0}$ *and* φ *is spherically symmetric about* $\mathbf{s}_0$*.*

Example 3. *Second-order intensity-reweighted isotropic (SOIRI) SPPs. The second-order intensity function of a SOIRI SPP* $\mathcal{N}$ *can be expressed as* $\lambda_2(\mathbf{s}_1,\mathbf{s}_2) = [g(\|\mathbf{s}_1-\mathbf{s}_2\|)-1]\lambda(\mathbf{s}_1)\lambda(\mathbf{s}_2)$*. If* $\mathcal{N}$ *is first-order spherically symmetric, then there exists an* $\mathbf{s}_0 \in \mathbb{R}^d$*, such that for any orthogonal matrix* $\mathbf{U}$*, we have* $\lambda_2(\mathbf{s}_0+\mathbf{U}(\mathbf{s}_1-\mathbf{s}_0),\mathbf{s}_0+\mathbf{U}(\mathbf{s}_2-\mathbf{s}_0)) = [g(\|(\mathbf{s}_0+\mathbf{U}(\mathbf{s}_1-\mathbf{s}_0))-(\mathbf{s}_0+\mathbf{U}(\mathbf{s}_2-\mathbf{s}_0))\|)-1]\lambda(\mathbf{s}_0+\mathbf{U}(\mathbf{s}_1-\mathbf{s}_0))\lambda(\mathbf{s}_0+\mathbf{U}(\mathbf{s}_2-\mathbf{s}_0)) = [g(\|\mathbf{s}_1-\mathbf{s}_2\|)-1]\lambda(\mathbf{s}_1)\lambda(\mathbf{s}_2)$*, implying that* $\mathcal{N}$ *is also second-order spherically symmetric.*

Example 4. *The epidemic-type aftershock sequence (ETAS) model. The ETAS model is one of the most important models in the analysis of earthquake clusters. It is defined by a conditional intensity function only affected by ancestors (i.e., mainshocks), but not offspring (i.e., aftershocks). If an extremely large mainshock earthquake occurs, then within a short period, the ETAS model is dominated by its aftershock patterns. Let the magnitude and the spatiotemporal location of the*

Statistica Sinica: Preprint
doi:10.5705/ss.202018.0214

extremely large mainshock earthquake be denoted by M^* *and* $(\mathbf{s}^*, t^*)$*, respectively. The conditional intensity function can be approximated by*

$$\lambda^*(\mathbf{s}, t, M) = j(M)\nu(M^*)u(t - t^*)v(\mathbf{s} - \mathbf{s}^*|M^*), \tag{4}$$

where $v(\cdot|M^*)$ *is modeled by a spherically symmetric function at the beginning (Zhuang, Ogata, and Vere-Jones, 2002), and later by an elliptically symmetric function (Ogata and Zhuang, 2006). If a spherically symmetric* $v(\cdot|M^*)$ *is adopted, then the aftershock pattern of earthquake locations can be roughly represented by a spherically symmetric Poisson SPP, indicating that it is strongly spherically symmetric.*

Motivated by the above examples, we find that it is important to justify the first-order spherical symmetry, in practice. If an SPP is first-order spherically symmetric, then with a few weak assumptions, it may also be second-order spherically symmetric, and even strongly spherically symmetric. Therefore, we propose a testing method to assess the first-order spherically symmetry.

2.3 A Test for Spherical Symmetry

We propose a Kolmogorov–Smirnov test to assess spherical symmetry. The test is conveniently modified from the classical Kolmogorov–Smirnov test for multivariate distributions. Let $\mathbf{y}$ be a continuous random vector on $\mathbb{R}^p$, with a joint CDF F. To test a null hypothesis $\mathcal{H}_0 : F = F_0$, the Kolmogorov–Smirnov statistic for

Statistica Sinica: Preprint
doi:10.5705/ss.202018.0214

multivariate distributions is given by $K_n = \sup_{\mathbf{y}\in\mathbb{R}^p} \sqrt{n}|\hat{F}(\mathbf{y}) - \hat{F}_0(\mathbf{y})|$, where n is the sample size, $\hat{F}$ is the sample CDF, and $\hat{F}_0$ is the sample CDF under $\mathcal{H}_0$. If data are collected identically and independently, then K_n converges weakly to the absolute value of a certain functional Brownian sheet, the distribution of which may depend on F_0. Because neither the exact nor the approximate ways are available, a simulation method is often used to compute the p-value of the test.

Without loss of generality, we assume that $\kappa = \int_{\mathbb{R}^d} \lambda(\mathbf{s})d\mathbf{s} < \infty$ and $\mathbf{s}_0 = \mathbf{0}$. We can restrict our method in $\{\mathbf{s} : \|\mathbf{s}\| \le \eta\}$ for a certain $\eta \in \mathbb{R}^+$ if $\kappa = \infty$. We can make a location shift of coordinates of points if $\mathbf{s}_0 \neq 0$. Then, $\mathcal{N}$ is first-order spherically symmetric if and only if $\lambda(\mathbf{s}) = \lambda_0(r)$, where $\lambda_0(r)$ is the mean of $\lambda(\mathbf{s})$ on the sphere $\{\mathbf{s} : \|\mathbf{s}\| = r\}$. We study a hypothesis testing problem for

$$\mathcal{H}_0 : \lambda(\mathbf{s}) = \lambda_0(\|\mathbf{s}\|), \forall\ \mathbf{s} \in \mathbb{R}^d \tag{5}$$

against

$$\mathcal{H}_1 : \exists\ \mathbf{s} \in \mathbb{R}^d, \text{s.t. } \lambda(\mathbf{s}) \neq \lambda_0(\|\mathbf{s}\|). \tag{6}$$

Let $(z_\mathbf{s}, \boldsymbol{\beta}_\mathbf{s})$ be the polar coordinates of $\mathbf{s}$, where $z_\mathbf{s} \in \mathbb{R}^+$ is the length and $\boldsymbol{\beta}_\mathbf{s} = (\beta_1, \cdots, \beta_{(d-1)})^\top \in \Theta = [0,\pi]^{d-2} \times [0, 2\pi]$ is the angle vector of $\mathbf{s}$. Let $f(\mathbf{s}) = \lambda(\mathbf{s})/\kappa$, $f_0(\mathbf{s}) = \lambda_0(z_\mathbf{s})/\kappa$, $F(r, \boldsymbol{\theta}) = \int_{z_\mathbf{s}\le r, \boldsymbol{\beta}_\mathbf{s} \preceq \boldsymbol{\theta}} f(\mathbf{s})d\mathbf{s}$, and $F_0(r, \boldsymbol{\theta}) = \int_{z_\mathbf{s}\le r, \boldsymbol{\beta}_\mathbf{s} \preceq \boldsymbol{\theta}} f_0(\mathbf{s})d\mathbf{s}$, for $r \in \mathbb{R}^+$ and $\boldsymbol{\theta} = (\theta_1, \cdots, \theta_{d-1})^\top \in \Theta$, where $\boldsymbol{\beta} \preceq \boldsymbol{\theta}$ means

Statistica Sinica: Preprint
doi:10.5705/ss.202018.0214

that $\boldsymbol{\beta}$ precedes $\boldsymbol{\theta}$, which holds if and only if $\beta_j \le \theta_j$, for all $j = 1, \cdots, d$. Then, $f(r, \boldsymbol{\theta})$ and $f_0(r, \boldsymbol{\theta})$ are probability density functions (PDFs) and $F(r, \boldsymbol{\theta})$ and $F_0(r, \boldsymbol{\theta})$ are cumulative distribution functions (CDFs) of r and $\boldsymbol{\theta}$.

Let $A_r = \{\mathbf{s} : z_{\mathbf{s}} \le r\}$ and $B_{\boldsymbol{\theta}} = \{\mathbf{s} : \boldsymbol{\beta}_{\mathbf{s}} \preceq \boldsymbol{\theta}\}$. Then, $A_r \cap B_{\boldsymbol{\theta}} = \{\mathbf{s} : z_{\mathbf{s}} \le r, \boldsymbol{\beta}_{\mathbf{s}} \preceq \boldsymbol{\theta}\}$ is a bounded sector region in $\mathbb{R}^d$. For any $\boldsymbol{\theta} \in \Theta$, $F(r, \boldsymbol{\theta})$ and $F_0(r, \boldsymbol{\theta})$ are the expected proportions of points in $A_r \cap B_{\boldsymbol{\theta}}$ under $\mathcal{H}_0 \cup \mathcal{H}_1$ and $\mathcal{H}_0$, respectively, given that they are in A_r. Our Kolmogorov–Smirnov–type statistic is constructed based on the maximum absolute difference between the estimators of $F(r, \boldsymbol{\theta})$ and $F_0(r, \boldsymbol{\theta})$.

Let $a_d(\boldsymbol{\theta})$ be the Lebesgue measure of $\{\boldsymbol{\theta}' \in \Theta : \boldsymbol{\theta}' \preceq \boldsymbol{\theta}\}$ proportional to the Lebesgue measure of Θ. Then, $a_d(\boldsymbol{\theta})$ is the CDF of the uniform distribution on Θ. With a few steps of integral calculations, we have $a_d(\boldsymbol{\theta}) = |\Theta|^{-1} \prod_{j=1}^{d-2} c_j(\theta_j)$, where $|\Theta| = 2\pi^{d/2}/\Gamma(d/2)$,

$$c_j(t) = \begin{cases} \text{Beta}(\sin^2 t; \frac{d-j+1}{2}, \frac{1}{2})/2, & 0 \le t \le \pi/2, \\ \text{Beta}(\frac{d-j+1}{2}, \frac{1}{2}) - \text{Beta}(\sin^2 t; \frac{d-j+1}{2}, \frac{1}{2})/2, & \pi/2 < t \le \pi, \end{cases}$$

for $j = 1, \cdots, d-2$, $c_{d-1}(t) = t$ for $t \in [0, 2\pi]$, $\text{Beta}(u, v) = \Gamma(u)\Gamma(v)/\Gamma(u+v)$ is the Beta function, and $\text{Beta}(t; u, v) = \int_0^t z^{u-1}(1-z)^{v-1} dz$ is the incomplete Beta function. Thus, we have the following theorem; the proof is given in the online Supplementary Material.

Theorem 1. *Suppose that $F(r, \boldsymbol{\theta})$ is absolutely continuous with respect to the*

Statistica Sinica: Preprint
doi:10.5705/ss.202018.0214

Lebesgue measure. The necessary and sufficient condition for (5) to hold is that there exists a function $u(r)$ of r, such that

$$F(r, \boldsymbol{\theta}) = a_d(\boldsymbol{\theta})u(r) \tag{7}$$

holds, for all $r \in \mathbb{R}^+$ and $\boldsymbol{\theta} \in \Theta$.

Theorem 1 suggests a convenient way for us to propose our test. If we can successfully estimate $F(r, \boldsymbol{\theta})$ and $u(r)$, then we can assess $\mathcal{H}_0$ by testing (7). Because $\mathrm{E}[N(A_r \cap B_{\boldsymbol{\theta}})]/\kappa = F(r, \boldsymbol{\theta})$ and $\mathrm{E}[N(A_r)]/\kappa = u(r)$, $\mathcal{H}_0$ becomes $\mathrm{E}[N(A_r \cap B_{\boldsymbol{\theta}})] = a_d(\boldsymbol{\theta})\mathrm{E}[N(A_r)]$, for all $r \in \mathbb{R}^+$ and $\boldsymbol{\theta} \in \Theta$. Our test statistic has the form

$$T_{d,\xi} = \frac{1}{\xi\sqrt{N}} \sup_{r \in \mathbb{R}^+, \boldsymbol{\theta} \in \Theta} |N(A_r \cap B_{\boldsymbol{\theta}}) - a_d(\boldsymbol{\theta})N(A_r)|, \tag{8}$$

where ξ is an appropriate scaling term that ensures that the test statistic has a standard asymptotic null distribution. Our asymptotic results provide an estimator of ξ^2 as

$$\hat{\xi}^2 = \frac{1}{K-1} \sum_{i=1}^{K} \frac{[N(B_{\Theta_i}) - \hat{N}(B_{\Theta_i})]^2}{\hat{N}(B_{\Theta_i})}, \tag{9}$$

where $B_{\Theta_i} = \{(r, \boldsymbol{\theta}) : \boldsymbol{\theta} \in \Theta_i\}$, $N(B_{\Theta_i})$ is the observed number of points in B_{Θ_i}, $\hat{N}(B_{\Theta_i}) = (|\Theta_i|/|\Theta|)N$ is the estimated number of points in B_{Θ_i}, and $\{\Theta_1, \cdots, \Theta_K\}$ is a partition of Θ. Replacing ξ with $\hat{\xi}$, we obtain

$$T_d = T_{d,\hat{\xi}} = \frac{1}{\hat{\xi}\sqrt{N}} \sup_{r \in \mathbb{R}^+, \boldsymbol{\theta} \in \Theta} |N(A_r \cap B_{\boldsymbol{\theta}}) - a_d(\boldsymbol{\theta})N(A_r)|. \tag{10}$$

Statistica Sinica: Preprint
doi:10.5705/ss.202018.0214

We show in Section 2.4 (i.e., Theorem 3) that the null distribution of T_d can be approximated by the distribution of $\|\mathbb{G}_d\|_\infty = \sup_{(r,\boldsymbol{\theta})\in[0,1]\times\Theta} |\mathbb{G}_d(r,\boldsymbol{\theta})|$, where $\mathbb{G}_d$ is a zero mean Gaussian process on $[0,1]\times\Theta$, with a covariance function given by

$$\mathrm{E}\{\mathbb{G}_d[(r,\boldsymbol{\theta})]\mathbb{G}_d[(r',\boldsymbol{\theta}')]\} = (r\wedge r')[a_d(\boldsymbol{\theta}\wedge\boldsymbol{\theta}') - a_d(\boldsymbol{\theta})a_d(\boldsymbol{\theta}')]. \tag{11}$$

We reject $\mathcal{H}_0$ at the α significance level if $T_d > \|\mathbb{G}_d\|_{\alpha,\infty}$, where $\|\mathbb{G}_d\|_{\alpha,\infty}$ is the upper α-quantile of the distribution of $\|\mathbb{G}_d\|_\infty$. By a Monte Carlo method, we have $\|\mathbb{G}_2\|_{0.1,\infty} = 1.2937$, $\|\mathbb{G}_2\|_{0.05,\infty} = 1.4250$, and $\|\mathbb{G}_2\|_{0.01,\infty} = 1.6918$, which are used to test for spherical symmetry by T_2. We also have $\|\mathbb{G}_3\|_{0.1,\infty} = 1.5896$, $\|\mathbb{G}_3\|_{0.05,\infty} = 1.7184$, and $\|\mathbb{G}_3\|_{0.01,\infty} = 1.9719$, which are used to test for spherical symmetry by T_3. In particular, we use $\|\mathbb{G}_2\|_{0.05,\infty}$ and $\|\mathbb{G}_2\|_{0.05,\infty}$ in our simulation studies (i.e., Section 3) to verify the asymptotic null distributions. We use $\|\mathbb{G}_2\|_{0.05,\infty}$ and the simulated distribution of $\|\mathbb{G}_d\|_\infty$ for the significance and the p-value, respectively, of the test in our analysis of an earthquake data set (see Section 4).

We specify T_d for $d = 2$ and $d = 3$, and numerically evaluate the values of $\|\mathbb{G}\|_{\alpha,\infty}$ using Monte Carlo methods. If $d = 2$, then $a_2(\boldsymbol{\theta}) = \theta/(2\pi)$, where $\boldsymbol{\theta} = \theta \in [0, 2\pi]$, indicating that

$$T_2 = \frac{1}{\hat{\xi}\sqrt{N}} \sup_{r\in\mathbb{R}^+,\theta\in[0,2\pi]} |N(A_r\cap B_\theta) - N(A_r)\theta/(2\pi)|. \tag{12}$$

If $d = 3$, then $a_3(\boldsymbol{\theta}) = (1-\cos\theta_1)\theta_2/(4\pi)$, where $\boldsymbol{\theta} = (\theta_1,\theta_2) \in [0,\pi]\times[0,2\pi]$,

Statistica Sinica: Preprint
doi:10.5705/ss.202018.0214

indicating that

$$T_3 = \frac{1}{\hat{\xi}\sqrt{N}} \sup_{r\in\mathbb{R}^+,\theta_1\in[0,\pi],\theta_2\in[0,2\pi]} |N(A_r \cap B_{\boldsymbol{\theta}}) - N(A_r)(1-\cos\theta_1)\theta_2/(4\pi)|. \quad (13)$$

Although T_d is presented on the entire space, it can be modified to a bounded region $W \subseteq \mathbb{R}^d$. If there exists an η, such that $A_\eta \subseteq W$, then we can restrict $N(A_r \cap B_{\boldsymbol{\theta}})$ and $N(A_r)$ in (10) within A_η, indicating that the supremum of T_d is computed under $r \in [0, \eta]$ and $\boldsymbol{\theta} \in \Theta$. In practice, we need to use the largest η satisfying $A_\eta \subseteq W$. We modify observations of the point process by excluding points outside of A_η. To be consistent, we need to modify $\lambda(\mathbf{s})$ by setting $\lambda(\mathbf{s}) = 0$ if $\mathbf{s} \notin A_\eta$. If we define $\kappa = \mathrm{E}[N(A_\eta)]$, then we still have $\kappa < \infty$ and a modified T_d is defined. This problem is considered in our simulation studies.

2.4 Asymptotic Distribution

We provide the asymptotic null distribution and power function of T_d under the framework of increasing domain asymptotics with weak dependence. For a bounded observed region W_η of the point pattern, the framework studies the asymptotics under the condition that $|W_\eta| \to \infty$ as $\eta \to \infty$. This approach has been widely adopted in many previous articles. Examples include Guan and Loh (2007), Guan and Shen (2010), Waagepetersen and Guan (2009), Guan, Jalilian, and Waagepetersen (2015), Prekešová and Jensen (2013), and Schoenberg (2005).

Statistica Sinica: Preprint
doi:10.5705/ss.202018.0214

The weak dependence is described by the strong mixing condition. Let $\mathscr{B}(E)$ be the collection of Borel sets generated by E. Denote the diameter of E by $\rho(E)$ and the minimum distance between E_1 and E_2 by $\rho(E_1, E_2)$, where $\rho(E) = \sup_{\mathbf{s},\mathbf{s}'\in E} \|\mathbf{s}-\mathbf{s}'\|$ and $\rho(E_1, E_2) = \min_{\mathbf{s}\in E_1,\mathbf{s}'\in E_2} \|\mathbf{s}-\mathbf{s}'\|$. Let

$$\alpha(u, v) = \sup\{|P(U_1 \cap U_2) - P(U_1)P(U_2)| : U_1 \in \mathscr{B}(E_1), U_2 \in \mathscr{B}(E_2),$$
$$\rho(E_1, E_2) \geq u, \rho(E_1) \leq v, \rho(E_2) \leq v, E_1, E_2 \in \mathscr{B}(W_\eta)\}$$

be the mixing coefficients, where $P(U)$ is generated by the distribution of $N(U)$. We say that $\mathcal{N}$ is *strongly mixing* if $\alpha(hu, hv) \to 0$ as $h \to \infty$, for any $u, v > 0$.

To control the performance of W_η as $\eta \to \infty$, one often assumes that $W_\eta = \eta W = \{\eta\mathbf{s} : \mathbf{s} \in W\}$, where W is a fixed measurable subset of $\mathbb{R}^d$. Without loss of generality, we assume that $W = \{\mathbf{s} : \|\mathbf{s}\| \leq 1\}$ and only points in $W_\eta = \{\mathbf{s} : \|\mathbf{s}\| \leq \eta\}$ are observed. The results of the asymptotics rely on properties of $\phi_\eta(C, D) = \pi(A_C \cap B_D) - a_D\pi_\eta(A_C)$ for $C \subseteq [0, 1]$ and $D \subseteq \Theta$, where $A_C = \{\mathbf{s} : z_\mathbf{s} \in C\}$, $B_D = \{\mathbf{s} : \boldsymbol{\beta}_\mathbf{s} \in D\}$, $\pi(E) = \pi_\eta(E) = \mathrm{E}[N_\eta(E)]/\kappa_\eta$, and $N_\eta(E) = N(\eta E)$, for any $E \in \mathscr{B}(W)$, $\kappa_\eta = \mathrm{E}(N_\eta)$, and $N_\eta = N(W_\eta)$. If $\mathcal{H}_0$ holds, then $\phi_\eta(C, D) = 0$; otherwise, there exist $C \in \mathscr{B}(W)$ and $D \in \mathscr{B}(\Theta)$, such that $\phi_\eta(C, D) \neq 0$. The primary issue is to show the functional central limit theorem of

$$M_\eta(E) = \eta^{-d/2}\{N_\eta(E) - \mathrm{E}[N_\eta(E)]\}, E \subseteq W,$$

under a few scenarios of $\phi_\eta(C, D)$ when $\eta \to \infty$. These provide the asymptotic

Statistica Sinica: Preprint
doi:10.5705/ss.202018.0214

null distribution, consistency, and local consistency of T_d. We prove the conclusions using the standard method, initially introduced by Ibragimov (1962), and later modified by Herrndorf (1984). The idea is to split any $E \subseteq W$ into two collections of subsets, say $\mathcal{C}$ and $\mathcal{D}$. Both $\mathcal{C}$ and $\mathcal{D}$ can be written as the sum of blocks, where the counts in blocks of $\mathcal{C}$ are almost independent, and the counts in blocks of $\mathcal{D}$ can be ignored. This is a popular idea in the proof of the functional central limit theorem under weak dependence. We only state the theorems here. The proofs of the theorems are given in the online Supplementary Material.

Theorem 2. *Assume that $\mathcal{N}$ is strongly mixing and there exist positive c_1 and c_2 such that $c_1 \leq \lambda(\mathbf{s}) \leq c_2$, for all $\mathbf{s}$. If the fourth-order intensity function of $\mathcal{N}$ is uniformly bounded and*

$$\int_0^\infty h^{d-\frac{1}{2}} \alpha(hu, hv) dh < \infty, \tag{14}$$

for any positive u and v, then $M_\eta(\cdot)$ converges weakly to a mean zero Gaussian process with independent increments, and there exists a measure ν on W such that $\{M_\eta(A_r \cap B_{\boldsymbol{\theta}}) : r \in [0,1], \boldsymbol{\theta} \in \Theta\}$ converges weakly to a d-dimensional mean zero Gaussian process $\mathbb{B}_\nu(\mathbf{t})$, with a covariance function given by

$$\mathrm{E}[\mathbb{B}_\nu(\mathbf{t}_1)\mathbb{B}_\nu(\mathbf{t}_2)] = \nu(A_{r_1 \wedge r_2} \cap B_{\boldsymbol{\theta}_1 \wedge \boldsymbol{\theta}_2}),$$

where $\mathbf{t}_i = (r_i, \theta_{i1}, \cdots, \theta_{i(d-1)}) \in W$, for $i = 1, 2$. If there also exists a constant

Statistica Sinica: Preprint
doi:10.5705/ss.202018.0214

ω^2, such that

$$\omega^2 = \lim_{\eta\to\infty} \int_{W_\eta} [g(\mathbf{s}, \mathbf{s}') - 1]\lambda(\mathbf{s}')d\mathbf{s}',$$

then $\nu = \xi\mu$, where $\xi = 1 + \omega^2$ and μ is the mean measure generated by the first-order intensity function of $\mathcal{N}$.

Theorem 3. *(Asymptotic null distribution). Suppose that all assumptions of Theorem 2 and $\mathcal{H}_0$ hold. Let $\mathbb{G}_d$ be a mean zero Gaussian process on $[0,1] \times \Theta$, with a covariance function given by (11). Then, $T_d \rightsquigarrow \|\mathbb{G}_d\|_\infty$.*

Theorem 4. *(Consistency). Suppose there exist $C \in \mathscr{B}([0,1])$ and $D \in \mathscr{B}(\Theta)$, such that $|\phi_\eta(C, D)|$ approaches a positive number as $\eta \to \infty$. For any consistent estimator $\hat{\xi}^2$ of ξ^2, if all assumptions of Theorem 2 hold, but $\mathcal{H}_0$ is violated, then $\lim_{\eta\to\infty} P(T_d \geq c\kappa_\eta^{1/2-\epsilon}) = 1$, for any positive ϵ and c.*

Theorem 5. *(Local consistency). Suppose that $\sup_{r\in[0,1],\boldsymbol{\theta}\in\Theta} |\kappa_\eta^{1/2}\phi_\eta(A_r, B_{\boldsymbol{\theta}})|$ goes to a bounded constant as $\eta \to \infty$. For any consistent estimator $\hat{\xi}^2$ of ξ^2, if all assumptions of Theorem 2 hold, but $\mathcal{H}_0$ is violated, then there exists a PDF $g(\cdot)$ satisfying $g(t) > 0$, for any $t \in \mathbb{R}^+$, such that $\lim_{\eta\to\infty} P(T_d < t) = \int_0^t g(u)du$ for any $t \in \mathbb{R}^+$.*

We provide conclusions about the asymptotic null distribution, consistency, and local consistency of our test in Theorems 3, 4, and 5, respectively. In particular, Theorem 3 points out that the p-value of the test can be approximately cal-

Statistica Sinica: Preprint
doi:10.5705/ss.202018.0214

culated by the distribution of $\|\mathbb{G}_d\|_\infty$, where $\mathbb{G}_d$ is a mean zero Gaussian process on $[0,1]\times\Theta$, with a covariance function given by (11). Theorem 4 points out that the power function of the test approaches one if $\sup_{C\in\mathscr{B}([0,1]),D\in\mathbb{B}(\Theta)}|\phi_\eta(C,D)|$ does not approach zero as $\eta\to\infty$. Note that $\lim_{\eta\to\infty}N_\eta/\kappa_\eta=1$. Together with Theorem 4, Theorem 5 points out that the optimal rate of the test under the alternative hypothesis is attained.

3. Simulation Studies

We carried out simulation studies to evaluate the performance of our testing method at the 0.05 significance level. We simulated realizations from Poisson and Poisson cluster SPPs in a bounded region $W_\eta=\{\mathbf{s}\in\mathbb{R}^d:\|\mathbf{s}\|\le\eta\}$, with a varied η. We selected these processes because they are popular in the modeling of ecological and environmental data. We evaluated the type-I error probabilities and the power functions of T_2 and T_3 as η varied. For a process in $W_\eta\subseteq\mathbb{R}^2$, we chose the first-order intensity function of $\mathcal{N}$ as $\lambda(\mathbf{s})=\kappa f_\rho(\mathbf{s})$, with $\rho\in[0,1)$ and $\mathbf{s}=(s_1,s_2)\in W_\eta$, where

$$f_\rho(\mathbf{s})=f_{2,\rho}(\mathbf{s})=\frac{1}{2(\eta/3)^2\pi\sqrt{1-\rho^2}}\exp\left\{-\frac{s_1^2-2\rho s_1s_2+s_2^2}{2(\eta/3)^2\pi(1-\rho^2)}\right\}. \qquad (15)$$

In (15), $f_\rho(\mathbf{s})$ was derived by restricting the density of the bivariate normal distribution on W_η, with both expected values equal to zero, both variances equal to $(\eta/3)^2$, and the correlation equal to ρ. For a process in $W_\eta\subseteq\mathbb{R}^3$, we chose

Statistica Sinica: Preprint
doi:10.5705/ss.202018.0214

$\lambda(\mathbf{s}) = \kappa f_\rho(\mathbf{s})$, where $f_\rho(\mathbf{s}) = f_{3,\rho}(\mathbf{s})$ was derived by restricting the density of the three-dimensional normal distribution on W_η, with all expected values equal to zero, all variances equal to $(\eta/3)^2$, and all correlations equal to ρ. Therefore, $\lambda(\mathbf{s})$ is spherically symmetric about $\mathbf{0}$ if and only if $\rho = 0$. We set $\kappa = 40\eta^2/9$, which is equivalent to $\eta = (9\kappa/40)^{1/2}$, such that κ varies with η.

We followed the standard way to generate Poisson and Poisson cluster SPPs (Guan, 2008, e.g). To obtain a Poisson SPP, we first generated the number of points from the $Poisson(\kappa)$ distribution. We then identically and independently generated the locations of these points from the distribution with density equal to $f_\rho(\mathbf{s})$. To obtain a Poisson cluster SPP, we first generated their parent points from a Poisson SPP, with its first-order intensify function equal to $\lambda_p(\mathbf{s}) = \lambda(\mathbf{s})/\gamma$. Then, we generated offspring points based on their corresponding parent points, where each parent point generated $Poisson(\gamma)$ offspring points independently. The position of each offspring point relative to its parent point was defined as a radially symmetric Gaussian random variable with a standard deviation σ. We chose $\gamma = 5$ and $\sigma = 0.02$ in all cases of Poisson cluster SPPs studied. We removed points outside of W_η.

We computed our test statistic for processes on $\mathbb{R}^2$ (i.e., in W_η with $d = 2$) and $\mathbb{R}^3$ (i.e., in W_η with $d = 3$). For a process on $\mathbb{R}^2$, we defined $A_r = \{\mathbf{s} : \|\mathbf{s}\| \leq r\}$ and $B_\theta = \{\beta : 0 \leq \beta \leq \theta\}$, for $r \in [0, \eta]$ and $\theta \in [0, 2\pi]$. For an individual

Statistica Sinica: Preprint
doi:10.5705/ss.202018.0214

$\mathbf{s}_i = (s_{i1}, s_{i2})$, we computed its Euclidean norm value using $\|\mathbf{s}_i\| = (s_{i1}^2 + s_{i2}^2)^{1/2}$, and its angle value using $\beta_i = \arccos(s_{i1}/\|\mathbf{s}_i\|) + \pi I(s_{i2} < 0)$. Then, we calculated $N(A_r \cap B_\theta) = \#\{\mathbf{s}_i : \|\mathbf{s}_i\| \le r, \beta_i \in [0, \theta]\}$ and $N(A_r) = \#\{\mathbf{s}_i : \|\mathbf{s}_i\| \le r\}$. We defined our test statistic as

$$T_2 = \frac{1}{\hat{\xi}\sqrt{N}} \sup_{r \in [0,\eta], \theta \in [0,2,\pi]} |N(A_r \cap B_\theta) - N(A_r)\theta/(2\pi)|,$$

where $\hat{\xi}$ was derived by (10) with $K = [N^{1/2}]$ (the highest integer not greater than $N^{1/2}$) equal partitions of $[0, 2\pi]$ based on the β_i values. We rejected $\mathcal{H}_0$ if $T_2 > 1.4250$, which was the value of $\|\mathbb{G}_2\|_{0.05,\infty}$ that we have derived via a Monte Carlo method.

For a process on $\mathbb{R}^3$, we defined $A_r = \{\mathbf{s} : \|\mathbf{s}\| \le r\}$ and $B_{\boldsymbol{\theta}} = \{\boldsymbol{\beta} = (\beta_1, \beta_2) : 0 \le \beta_1 \le \theta_1, 0 \le \beta_2 \le \theta_2\}$, for $r \in [0, \eta]$ and $\boldsymbol{\theta} = (\theta_1, \theta_2) \in [0, \pi] \times [0, 2\pi]$. For an individual $\mathbf{s}_i = (s_{i1}, s_{i2}, s_{i3})$, we computed its Euclidean norm value using $\|\mathbf{s}\| = (s_{i1}^2 + s_{i2}^2 + s_{i3}^2)^{1/2}$, and its angle vectors $\boldsymbol{\beta}_i = (\beta_{i1}, \beta_{i2})$ using $\beta_{i1} = \arccos(s_{i1}/\|\mathbf{s}\|)$ and $\beta_{i2} = \arccos[s_{i2}/(s_{i2}^2 + s_{i3}^2)^{1/2}] + \pi I(s_{i3} < 0)$. Then, we calculated the values of $N(A_r \cap B_{\boldsymbol{\theta}})$ and $N(A_r)$. We defined our test statistic as

$$T_3 = \frac{1}{\hat{\xi}\sqrt{N}} \sup_{r \in [0,\eta], \theta_1 \in [0,\pi], \theta_2 [0,2,\pi]} |N(A_r \cap B_\theta) - N(A_r)(1 - \cos\theta_1)\theta_2/(4\pi)|,$$

where $\hat{\xi}$ was also derived by (10) with $K = 2K_0^2$ and $K_0 = [N^{1/3}]$ equal partitions of $[0, \pi]$ and $[0, 2\pi]$, respectively, based on the values of β_{i1} and β_{i2}. We rejected $\mathcal{H}_0$ if $T_3 \ge 1.7184$, which was the value of $\|\mathbb{G}_3\|_{0.05,\infty}$ derived using a Monte Carlo

Statistica Sinica: Preprint
doi:10.5705/ss.202018.0214

method.

We simulated 1,000 realizations for each selected case. We obtained the type-I error probabilities and power functions of T_2 and T_3 (Table 1). The results show that the type-I error probabilities (i.e., when $\rho = 0$) are all close to 0.05, indicating that our asymptotic null distribution provides an appropriate way to test the significance. It also indicates that the asymptotic null distribution provided by Theorem 3 is accurate. The power values (i.e., when $\rho > 0$) increase as ρ increase, which is expected, because the strength of spherical asymmetry increases with ρ. For the same ρ-value, the power increases with κ. This is expected, because the expected number of points increases when κ becomes large. We find that the power values in the Poisson cluster SPPs are lower than those in the Poisson SPPs. This is because the performance of the power functions is controlled primarily by the intensity functions of the parent process. Because the expected number of parent points was much lower than the value of κ, they were lower than those simulated from the Poisson SPPs.

4. Application

We applied our test to an earthquake data set. Earthquakes are considered the most important natural hazard events that results in death and damage. This motivated us to apply our method to earthquake studies. Many sources of

Statistica Sinica: Preprint
doi:10.5705/ss.202018.0214

Table 1: Simulations (with 1,000 replications) for Type-I error probabilities ($\rho = 0$) and powers ($\rho > 0$) of T_2 and T_3 for selected κ on W_η, with $\eta = (9\kappa/40)^{1/2}$, at the 0.05 significance level in Poisson and (Poisson) cluster SPPs, respectively.

Test		ρ for Poisson Processes				ρ for Cluster Processes			
Statistic	κ	0.0	0.1	0.2	0.3	0.0	0.1	0.2	0.3
T_2	1,000	0.051	0.099	0.279	0.612	0.046	0.052	0.081	0.148
	2,000	0.045	0.197	0.682	0.976	0.040	0.076	0.145	0.321
	5,000	0.053	0.529	0.999	1.000	0.054	0.102	0.374	0.798
	10,000	0.052	0.898	1.000	1.000	0.053	0.206	0.764	0.997
T_3	1,000	0.053	0.111	0.539	0.933	0.042	0.061	0.076	0.124
	2,000	0.038	0.242	0.950	1.000	0.041	0.070	0.148	0.363
	5,000	0.055	0.774	1.000	1.000	0.053	0.111	0.458	0.889
	10,000	0.048	0.996	1.000	1.000	0.040	0.218	0.878	0.998

Statistica Sinica: Preprint
doi:10.5705/ss.202018.0214

earthquake databases have been established and are readily available via the Internet. Examples include the websites of the United States National Geophysical (USGS) data center, the Northern California Earthquake Data Center (NCEDC), and many others. These databases contain the time and date, depth, locations (given in longitude and latitude), and magnitudes, at either the regional or the global level, for the past several hundreds years.

A critical issue in the analysis of earthquake data is to address the impact of earthquake clusters caused by aftershocks. The presence of earthquake clusters often makes it difficult to understand the overall patterns of earthquake activities. Many statistical models have been proposed to account for earthquake clusters. Among these, the ETAS model has gained much attention and been applied extensively in recent years. The ETAS model is specified by a conditional intensity function. It models the occurrences of offspring (i.e, aftershocks) by clusters triggered by their corresponding ancestors (i.e., mainshocks). Using $(\mathbf{s}_k^*, t_k^*, M_k^*)$ to represent individual mainshock earthquakes, the ETAS model expresses its conditional intensity function for aftershock earthquakes as

$$\lambda(\mathbf{s}, t, M|\mathcal{H}_t) = j(M)[\mu(\mathbf{s}) + \sum_{k:t_k<t} \nu(M_k^*)u(t-t_k^*)v(\mathbf{s}-\mathbf{s}_k^*|M_k^*)],$$

where $j(M)$ is the standardized term, $\mu(\mathbf{s})$ is the background intensity function, $\mathcal{H}_t$ represents the history of mainshock earthquakes that occurred before the current time t, and $\nu(M_k^*)$ is the expected number of aftershocks from a main-

Statistica Sinica: Preprint
doi:10.5705/ss.202018.0214

shock ancestor. If an extremely large mainshock earthquake occurs within a short period, the performance of the ETAS model is dominated by its aftershock earthquakes, implying that the conditional intensity function can be approximately expressed as (4). Because the ETAS model assumes that each mainshock earthquakes produces aftershock earthquakes independently, aftershock occurrences caused by an extremely large mainshock earthquake can be treated as an approximately Poisson marked point process (MPP), with the first-order intensity function $\lambda^*(\mathbf{s}, t, M)$, given by (4). If $v(\mathbf{s} - \mathbf{s}^*|M^*) = v(\|\mathbf{s} - \mathbf{s}^*\|M^*)$, then $\lambda^*(\mathbf{s}, t, M)$ is spherically symmetric in the spatial domain. Therefore, we can test spherical symmetry by considering the spatial locations of the occurrences only. Because spatial spherical symmetry is often used as an assumption of the ETAS model, our test is important in the justification of the model. Because earthquake hazard maps often fail (Stein, Geller, and Liu, 2012), our test can provide another way to understand earthquake mechanisms.

We collected historical earthquake data from the NCEDC website. We focused on Japan and its neighboring Pacific Ocean regions because this is considered the most risky area earthquakes in the world. We studied earthquake occurrences after January 1, 2000, in these regions, and found that most earthquakes occurred in an area between 30°N and 45°N, and 130°E and 150°E. This area has been studied previously for earthquake occurrences (Zhang and Zhuang, 2014;

Statistica Sinica: Preprint
doi:10.5705/ss.202018.0214

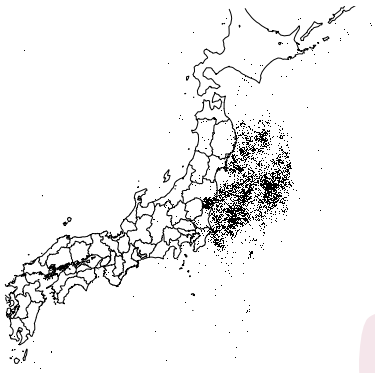

Figure 1: Aftershock earthquakes within the first 180 days of the *2011 Great Tohoku Earthquake*.

Zhang, 2017). Using this as the study area, we collected data on earthquake occurrences with magnitudes greater than or equal to 4.0 from January 1, 2000, to December 31, 2016. The data set contained 16,441 earthquakes, including 1,909 moderate (magnitude ≥ 5 but < 6), 201 strong (magnitude ≥ 6 but < 7), 20 major (magnitude ≥ 7 but < 8), and two great (magnitude ≥ 8) earthquakes. The most serious was the *Great Tohoku Earthquake*, which occurred in March 11, 2011, at 38.30°N 142.37°E with magnitude 9.1. It caused about 16,000 people deaths and a serious nuclear accident at the Fukushima Nuclear Power Plants, affecting hundreds of thousands of residents within a few thousand square kilometers of the disaster site.

Because the magnitude of the *2011 Great Tohoku Earthquake* was extremely

Statistica Sinica: Preprint
doi:10.5705/ss.202018.0214

large, we can use (4) to model its aftershock pattern. Note that M^*, t^*, and $\mathbf{s}^*$ are only related to the information of the mainshock earthquake. They can be treated as known constants in (4); therefore, the spatial margin of $\lambda^*(\mathbf{s}, t, M)$ becomes

$$\lambda(\mathbf{s}) = \kappa v(\mathbf{s} - \mathbf{s}^*|M^*), \tag{16}$$

where $\kappa = \nu(M^*) \int_0^\infty j(M)dM \int_0^\infty u(t - t^*)dt$. Thus, $\lambda^*(\mathbf{s}, t, M)$ is spherical symmetric if and only if $\lambda(\mathbf{s})$ is spherical symmetric about $\mathbf{s}^*$, indicating that we can employ $\mathbf{s}_0 = \mathbf{s}^*$ in our test.

We focused on earthquake aftershock activities within the first 180 days after the occurrence of the *Great Tohoku Earthquake*. The data set contained 4,503 earthquakes with magnitudes greater than or equal to 4.0, including zero great, four major, 73 strong, and 652 moderate earthquakes. We used T_2 to test the spherical symmetry of $\lambda(\mathbf{s})$ given by (16). To derive the value of T_2, we computed the spherical distance between the locations of the aftershocks and the mainshock earthquakes and the angles between the directions of the aftershock earthquakes and the mainshock earthquakes and the direction east. We also computed the value of $\hat{\xi}^2$ using the same method as that in our simulation studies. We calculated the p-value of T_2 based on the simulated distribution of $\|\mathbb{G}_2\|_\infty$. We rejected $\mathcal{H}_0$, concluding that the test is significant if $T_2 > 1.4250$, because the upper 0.05 quantile of the simulated distribution of $\|\mathbb{G}_2\|_\infty$ is 1.4250. We tested

Statistica Sinica: Preprint
doi:10.5705/ss.202018.0214

Table 2: Test for spherical symmetry of aftershock earthquakes within the first m days of the occurrence of the *Great Tohoku Earthquake*.

	Number of Aftershock Earthquakes					
m	Total	Major	Strong	Moderate	T_2	p-value
1	671	2	42	261	1.1088	0.2218
2	1,108	2	45	324	1.2688	0.1066
3	1,410	2	45	361	1.3684	0.0663
10	2,238	2	48	459	1.6928	0.0102
30	3,047	3	56	528	1.9090	0.0030
180	4,503	4	73	652	2.1782	0.0003

the spherical symmetry of the aftershock earthquakes within a few options of periods, starting from the occurrence of the *Great Tohoku Earthquake* (Table 2). We conclude that the spherical symmetry was correct, in general, at the beginning, but slightly violated at the end of the period. Based on our results, we conclude that the ETAS model is able to account for aftershock earthquake clusters in Japan and its neighboring areas.

Statistica Sinica: Preprint
doi:10.5705/ss.202018.0214

5. Discussion

We provide a Kolmogorov–Smirnov–type test to assess the first-order spherical symmetry of SPPs. The test is modified from the classical Kolmogorov–Smirnov test for multivariate distributions. The classical test is formulated under the assumption that sampling data are independently and independently collected. This assumption is violated because of the existence of dependence in spatial point data. We propose a way to account for this dependence using a dispersion parameter. Using our asymptotic theory, we present a method for approximately interpreting the dispersion parameter, using the well known quasi-Poisson model in the statistical literature, which provides an estimator of the parameter. Our test statistic is derived after the classical statistic is adjusted by the estimator of the dispersion parameter. Because our test statistic does not involve nonparametric smoothing techniques, our test is consistent with the optimal rate (i.e., Theorems 4 and 5). Therefore, our test is asymptotically more powerful than any other test involving nonparametric smoothing techniques. Our method can also be modified to the Cramér–von Mises-type approach.

An obvious advantage is that the asymptotic null distribution of our test statistic does not rely on the unknown underlying intensity function. It has been acknowledged that the asymptotic null distribution of an empirical statistic for multivariate distributions, such as the Kolmogorov–Smirnov or the Cramér–von

Statistica Sinica: Preprint
doi:10.5705/ss.202018.0214

Mises statistics, depends on the underlying distribution, making the computation of their asymptotical p-values complicated (Zhang and Zhuang, 2017). The asymptotic null distribution of a goodness-of-fit statistic in the one-dimensional case is often related to the distribution of a norm of the standard Brownian bridge, which may have a closed-form expression (van der Vaart, 1998, P. 297). This nice property makes it easy to implement goodness-of-fit tests for univariate distributions. Although the concept of the standard Brownian bridge has been extended to its high-dimensional version, called Brownian sheets, it is still difficult to implement goodness-of-fit tests for multivariate random variables, because neither the exact nor the approximate null distribution is available. Our research provides a way to implement this approach.

Testing the nice properties of intensity functions of SPPs is important, in practice. The problem studied in this article is only related to first-order spherical symmetry. It does not specify any second-order properties. Therefore, the selection of statistical models for the second-order properties is flexible. Because of the popularity of SOIRS, we can also model the second-order intensity function together with the first-order spherical symmetry, which provides a way to jointly analyze the first-order and second-order intensity functions. This is left to future research.

Statistica Sinica: Preprint
doi:10.5705/ss.202018.0214

Supplementary Material

The online Supplementary Material includes the proofs of Theorems 1, 2, 3, 4, and 5, as well as their associated lemmas.

Acknowledgements

The authors appreciate the comments of an associate editor and two anonymous referees, which significantly improved the quality of the article.

References

Baddeley, A.J., Møller, J. and Waagepetersen, R. (2000). Non- and semi-parametric estimation of interaction in inhomogeneous point patterns. *Statistica Neerlandica*, **54**, 329-350.

Balderama, E., Schoenberg, F.P., Murray, E., and Rundel, P.W. (2012). Application of branching models in the study of invasive species. *Journal of the American Statistical Association*, **107**, 467-476.

Besag, J. (1977). Contribution to the discussion of Dr. Ripley's paper. *Journal of the Royal Statistical Society Series B*, **39**, 193-195.

Brandwein, A.C., and Strawderman, W.E. (1991). Generalizations of James-Stein estimators under spherical symmetry. *Annals of Statistics*, **19**, 1639-1650.

Statistica Sinica: Preprint
doi:10.5705/ss.202018.0214

Daley, D.J. and Vere-Jones, D. (2003). *An Introduction to Theory of Point Processes: Volume I: Elementary Theory and Methods, Second Edition*. Springer, New York.

Diggle, P.J. (1985). A kernel method for smoothing point process data. *Applied Statistics*, **34**, 138-147.

Diggle, P.J. (2003). *Statistical Analysis of Spatial Point Patterns, 2nd Edition*, New York: Wiley.

Diggle, P.J. (2006). Spatio-temporal point processes, partial likelihood, foot and mouth disease. *Statistical Methods in Medical Research*, **16**, 325-336.

Guan, Y. and Loh, J.M. (2007). A thinned block bootstrap variance estimation procedure for inhomogeneous spatial point patterns. *Journal of the American Statistical Association*, **102**, 1377-1386.

Guan, Y. (2008). A KPSS test for stationarity for spatial point processes. *Biometrics*, **64**, 800-806.

Guan, Y. and Shen, Y. (2010). A weighted estimating equation approach for inhomogeneous spatial point processes. *Biometrika*, **97**, 867-880.

Guan, Y., Jalilian, A., Waagepetersen, R. (2015). Quasi-likelihood for spatial point processes. *Journal of Royal Statistical Society Series B*, **77**, 677-697.

Statistica Sinica: Preprint
doi:10.5705/ss.202018.0214

Hall, P., Watson, G.S., and Cabrera, J. (1987). Kernel density estimation with spherical data. *Biometrika*, **74**, 751-762.

Henrys, P.A. and Brown, P.E. (2009). Inference for cluster inhomogeneous spatial point processes. *Biometrics*, **65**, 423-430.

Henze, N., Hlávka, Z., and Meintanis, S.G. (2014). Testing for spherical symmetry via the empirical characetristic function. *Statistics*, **48**, 1282-1296.

Herrndorf, N. (1984). A functional central limit theorem for weakly dependent sequence of random variables. *Annals of Probability*, **12**, 141-153.

Ibragimov, I.A. (1962). Some limit theorems for stationary processes. *Stochastic Processes and Their Applications*, **12**, 171-186.

Janossy, L. (1950). On the absorption of a nucleon cascade. *Proceedings of the Royal Irish Academy A*, **53**, 181-888.

Justel, A., Peña, D., Zamar R. (1997). A multivariate Kolmogorov–Smirnov test of goodness of fit. *Statistics and Probability Letters*, **35**, 251-259.

Meyer, S. and Held, L. (2014). Power-law models for infectious disease spread. *Annals of Applied Statistics*, **8**, 1612-1639.

Møller, J. and Waagepetersen, R.P. (2007). Modern statistics for spatial point processes (with discussion). *Scandinavian Journal of Statistics*, **34**, 685-711.

Statistica Sinica: Preprint
doi:10.5705/ss.202018.0214

Moyal, J.E. (1962). The general theory of Stochastic population processes. *Acta Mathematics*, **108**, 1-31.

Myllymäki, M. and Penttinen, A. (2009). Conditionally heteroscedastic intensity-dependent marking of log Gaussian Cox processes. *Statistica Neerlandica*, **63**, 450-473.

Ogata, Y. (1988). Statistical models for earthquake occurrences and residual analysis for point processes. *Journal of the American Statistical Association*, **83**, 9-27.

Ogata, Y. and Zhuang, J. (2006). Space-time ETAS models and an improved extension. *Techonophysics*, **413**, 13-24.

Peng, R.D., Schoenberg, F.P, and Woods, J.A. (2005). A space-time conditional intensity model for evaluating a wildfire hazard index. *Journal of the American Statistical Association*, **100**, 26-35.

Prekešová, M. and Jensen, V.B.V. (2013). Asymptotic palm likelihood theory for stationary point processes. *Annals of Institute of Statistical Mathematics*, **65**, 387-412.

Ripley, B.D. (1976). The second-order analysis of spatial point processes. *Journal of Applied Probability*, **23**, 255-266.

Statistica Sinica: Preprint
doi:10.5705/ss.202018.0214

Schoenberg, F.P. (2005). Consistent parametric estimation of the intensity of a spatial-temporal point process. *Journal of Statistical Planning and Inference*, **128**, 79-93.

Stein, S., Geller, R.J., and Liu, M. (2012). Why earthquake hazard maps often fail and what to do about it. *Tectonophysics*, **562-563**, 046102.

Stoyan, D. and Stoyan, H. (1994). *Fractals, Random Shapes and Point Fields*. New York: Wiley.

Stoyan, D. and Stoyan, H. (1996). Estimating pair correlation functions of planar cluster processes. *Biometrical Journal*, **38**, 259-271.

van der Vaart, A.W. (1998). *Asymptotic Statistics*, Cambridge University Press, Cambridge, UK.

Waagepetersen, R. (2007). An estimating function approach to inference for inhomogeneous Neyman-Scott process. *Biometrics*, **63**, 252-258.

Waagepetersen, R. and Guan, Y. (2009). Two-step estimation for inhomogeneous spatial point processes. *Journal of the Royal Statistical Society B*, **71**, 685-702.

Zhang, T. and Zhuang, Q. (2014). On the local odds ratio between points and marks in marked point processes. *Spatial Statistics*, **9**, 20-37.

Statistica Sinica: Preprint
doi:10.5705/ss.202018.0214

Zhang, T. and Zhou, B. (2014). Test for stationarity for spatial point processes in an arbitrary region. *Journal of Agricultural, Biological and Environmental Statistics*, **19**, 387-404.

Zhang, T. (2014). A Kolmogorov–Smirnov type test for independence between marks and points of marked point processes. *Electronic Journal of Statistics*, **8**, 2557-2584.

Zhang, T. and Zhuang, R. (2017). Testing proportionality between the first-order intensity functions of spatial point processes. *Journal of Multivariate Analysis*, **155**, 72-82.

Zhang, T. (2017). On independence and separability between points and marks of marked point processes. *Statistica Sinica*, **27**, 207-227.

Zhuang, J., Ogata, Y., and Vere-Jones, D. (2002). Stochastic declustering of spacetime earthquake occurrences. *Journal of the American Statistical Association*, **97**, 369-380.